

## Photoinduced Charge Currents in Mesoscopic Rings

A. Matos-Abiague and J. Berakdar

Max-Planck Institut für Mikrostrukturphysik, Weinberg 2, 06120 Halle, Germany

(Received 3 January 2005; published 25 April 2005)

The temporal and spatial controllability of charge distribution in submicron structures opens new avenues for potential applications and for the understanding of nonequilibrium processes. Here we suggest a novel way to trigger and control within picoseconds charge currents and magnetic moments in nanoscopic and mesoscopic ring structures by applying two shaped, time-delayed light pulses. Our quantum dynamic calculations show that the magnitude and direction of the induced currents are tunable by varying the time delay and strengths of the pulses. Furthermore, in an array of rings desirable magnetic orders are generated depending on the ring sizes and particle number.

DOI: 10.1103/PhysRevLett.94.166801

PACS numbers: 73.23.-b, 42.65.Re, 73.21.-b, 78.67.-n

The interest of chemists and physicists in ringlike molecular and condensed matter systems dates back to the work of Kekulé's on the benzene molecular structure [1]. Since then, intriguing phenomena and potential applications have been unravelled [2], particularly when the size of these systems shrinks below the phase coherence length of their quantum states. In this case their low-temperature behavior becomes dominated by quantum interference effects. For example, when a ring structure is pierced by a magnetic flux  $\phi$  the ground state degeneracy with respect to clockwise and anticlockwise circular states is lifted; i.e., the state turns chiral, and a persistent charge current occurs [3,4]. Experiments [5–7] confirmed this effect. For ballistic structures [7], the emergence and the order of magnitude of the current derive from a consideration based on independent fermions confined in a one-dimensional ring of radius  $\rho_0$  pierced by  $\phi$  [8]. The single-particle stationary energies are  $E_{m_0} = \hbar^2 k_{m_0}^2 / 2m^*$ , with  $k_{m_0} = \frac{2\pi}{L} \times (m_0 - \frac{\phi}{\phi_0})$ . Here  $L = 2\pi\rho_0$  and  $m^*$  is the particle effective mass.  $m_0 = 0, \pm 1, \pm 2, \dots$  is the angular quantum number associated with the system's cylindrical symmetry around the ring normal.  $\phi_0 = hc/e$  is the flux quantum. The current follows from the flux dependence of the free energy and is typically on the order of few nanoamperes for micron-size ballistic rings in agreement with experiments [7]. To induce a ring chirality (i.e., to achieve  $E_{-m_0} \neq E_{+m_0}$ ) and hence a net current,  $\phi$  has to be comparable to  $\phi_0$ . When  $\rho_0$  (linearly) shrinks, the required magnetic field grows as  $\rho_0^2$ ; e.g., currents in a benzene-size ring cannot be generated with today's laboratory magnetic fields [9]. In addition, a temporal (picosecond) control of the current is not feasible due to the adiabatic switching of magnetic fields on the time scale of the current buildup. We therefore propose in this work a new way that utilizes light pulses to trigger chiral coherent states and hence dynamic currents in ring structures. As shown below, this method offers a possibility to control the magnitude and the time evolution of the induced current. The work is motivated by recent advances in the controlled fabrication of mesoscopic

and nanoscopic ring structures [10–12] and the impressive progress in generating and sculpturing precisely properties of light beams such as the fine-tuning of the amplitude, shape, and phase of electromagnetic pulses [13–20].

This work provides the first theoretical evidence that in the absence of magnetic fields, large charge currents and magnetization are generated and tunable within picoseconds in high purity GaAs-AlGaAs-based rings [7] upon applying two time-delayed, picosecond shaped electromagnetic pulses. Ordered magnetic states in ring arrays are controllably induced and modified. The employed pulses and ring structures are available experimentally.

The system under study is illustrated by Fig. 1: we consider the closed, isolated ballistic GaAs-AlGaAs-based ring with a width  $d$  and radius  $\rho_0$  that confines  $N$  independent charge carriers. Here  $d$  is in the range of 100 nm, whereas  $\rho_0$  is on the micrometer scale, i.e.,  $d \ll \rho_0$ . These rings are currently realizable [5,7]. Applying at  $t = t_1$  a time-asymmetric, linearly polarized electromagnetic pulse with an amplitude  $F_1(t)$  creates a nonequilibrium charge unbalance in the ring but does not destroy the clockwise-anticlockwise symmetry of the charge density. Hence, a charge polarization buildup occurs [21], but no net current flows. We note that the pulse asymmetry is vital

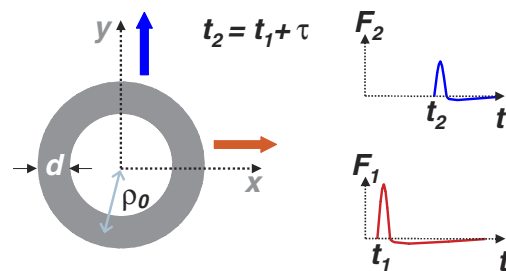


FIG. 1 (color online). A ballistic ring with a width  $d$  and a radius  $\rho_0 \gg d$  subjected to a sequence of two crossed time-asymmetric pulses applied at  $t = t_1$  and  $t = t_2 = t_1 + \tau$ . The pulses are linearly polarized along the perpendicular  $x$  and  $y$  axes.

for the polarization buildup. Time-symmetric (continuous wave) pulses do not generate a postpulse ring polarization [21]. The initial (field-free) energy levels  $E_{l_0, m_0}$  are classified according to  $m_0$  and  $l_0$  where  $l_0 = 1, 2, 3, \dots$  characterize the radial motion in the ring [21,22]. Since  $F_1$  is linearly polarized, the initial energy degeneracy with respect to  $m_0$  is preserved, i.e.,  $E_{l_0, m_0}(t) = E_{l_0, -m_0}(t)$  for all times [21]. A break of this symmetry is a prerequisite to trigger a net charge current. As outlined above, this symmetry break and hence the current are usually brought about by applying a (dc or ac) magnetic field *with* a static component [4–7,23–25]; we stress that the current diminishes when the static component vanishes. To generate currents in the absence of magnetic fields we illuminate the (polarized) ring by a second time-asymmetric pulse  $F_2(t)$ , as depicted in Fig. 1. Qualitatively speaking, the second pulse  $F_2(t)$ , acting at the time  $t_2$  after the first pulse  $F_1$ , kicks the charge density accumulated by  $F_1$  to result in a chiral coherent state [i.e.,  $E_{l_0, m_0}(t_2) \neq E_{l_0, -m_0}(t_2)$ ] and a net time-dependent current  $I(t > t_2)$ .

For thin ballistic rings in equilibrium, the independent carriers picture is appropriate for describing the system [2,7,26]. We consider weak pulses such that the system is not driven far from the equilibrium and, therefore, the noninteracting model is still appropriate [21]. In a more general case the interaction among the carriers could be included in a mean field approximation [27]. Thus, to predict the ring response to the applied pulses we study the single-particle, time-dependent wave functions  $\Psi_{l_0, m_0}(\rho, \theta, t)$ . Here the parametric dependence on  $l_0, m_0$  signifies the initial condition that for  $t < t_1$  the particle occupies the stationary state labeled by  $l_0, m_0$ .  $\theta(\rho)$  specifies the particle angular (radial) position with respect to the

$x$  axis in Fig. 1. To obtain  $\Psi_{l_0, m_0}(\rho, \theta, t)$  we solve for the nonrelativistic, time-dependent Schrödinger equation in the presence of the pulses and the confining potential  $V_c(\rho)$ .  $V_c$  vanishes inside the ring and is infinitely large otherwise. In all cases shown below we employ two sine-square unipolar pulses each having a duration of 1 ps. The first (second) pulse is linearly polarized along the  $x$  ( $y$ ) axis (cf. Fig. 1). We investigate then the current dependencies on the time delay  $\tau$  and the values of the electric field amplitudes  $F_1$  and  $F_2$ , as well as on the number  $N$  of particles and  $\rho_0$ , where  $N \in [400, 1800]$ ,  $\rho_0 \in [800 \text{ nm}, 1400 \text{ nm}]$ ,  $d = 160 \text{ nm}$ , and  $m^* = 0.067m_e$  ( $m_e$  is the electron mass).

To inspect how strongly the system is disturbed, we trace the time evolution of the energy  $E_{l_0, m_0}(t)$  of a particle that developed from the stationary states  $l_0, m_0$ . This is achieved by computing the matrix elements  $E_{l_0, m_0}(t) = i\hbar \langle \Psi_{l_0, m_0}(\rho, \theta, t) | \frac{\partial}{\partial t} | \Psi_{l_0, m_0}(\rho, \theta, t) \rangle$ . The energy dependence on  $(l_0, m_0)$  is shown in Fig. 2(a) for different time intervals. From Fig. 2 it is evident that for the pulses considered here the system is only slightly perturbed. This is also evident by inspecting [as done in Figs. 2(b)–2(d)] the time-dependent change in the structure of the energy levels near the Fermi energy ( $E_F \approx 4.228 \text{ meV}$ ) on an enlarged scale. Comparing Figs. 2(b) and 2(c) we deduce that the action of the first pulse results in a small shift of the energy levels while preserving the initial energy degeneracy with respect to  $\pm m_0$ , meaning that the clockwise and anticlockwise circulating particle waves are energetically equivalent. This degeneracy is lifted upon applying the second pulse [cf. Fig. 2(d)] rendering thus a total current circulating in the ring. The total current generated in the ring is calculated as the weighted sum over all contributions of the partial currents  $I_{l_0, m_0}$  generated by the individual particles initially residing in the state specified by  $l_0, m_0$ , i.e.,  $I(t) = \sum_{l_0, m_0} \sigma f(l_0, m_0, \sigma, N, T, t) I_{l_0, m_0}(t)$ . Here  $\sigma$  stands for the spin of the particles and  $T$  is the temperature.  $f$  is the nonequilibrium distribution function of the charge carriers which we obtain from the Boltzmann equation using the relaxation time approximation [28] (in the examples shown here an averaged relaxation time of 25 ps is assumed). Since the rings are isolated and the fields are weak, the number of particles  $N$  is constant. The current carried by a particle initially occupying the stationary state  $(l_0, m_0)$  is  $I_{l_0, m_0}(t) = \int_{\rho_0 - d/2}^{\rho_0 + d/2} \times \int_0^{2\pi} j_{l_0, m_0}(\rho, \theta, t) \rho d\theta d\rho$  where  $j_{l_0, m_0}(\rho, \theta, t)$  is the current density associated with the wave function  $\Psi_{l_0, m_0}(\rho, \theta, t)$  that we determined by solving the corresponding Schrödinger equation.

Upon the two-pulse irradiation a current is generated, which in turn induces a time-dependent field-free magnetization  $M(t)$ . For rings with  $d \ll \rho_0$  this dynamic magnetization is  $M(t) \approx \pi \rho_0^2 I(t)$ . The magnetic flux generated at the axis of the ring by the initiated current is  $\Phi(t) \approx \frac{\pi}{2} \mu \rho_0 I(t)$  and  $\mu$  is the magnetic susceptibility of the

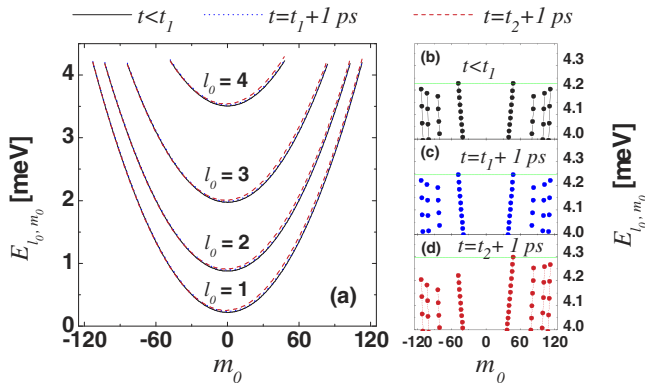


FIG. 2 (color online). (a) Calculated energy levels for different time intervals. The ring contains 1400 particles. The stationary Fermi energy is  $E_F \approx 4.228 \text{ meV}$ . The 1 ps long pulses have the amplitude strengths  $F_1 = F_2 = 100 \text{ V/cm}$  and are delayed by  $\tau = 15 \text{ ps}$ . Solid lines correspond to the equilibrium configuration before applying the pulses ( $t < t_1$ ). Dotted and dashed lines correspond, respectively, to the times after applying the first ( $t = t_1 + 1 \text{ ps}$ ) and the second ( $t = t_2 + 1 \text{ ps}$ ) pulses. (b)–(d) Zooms in (a) near  $E_F$ . The horizontal lines indicate the energy of the highest excited state.

surrounding material. Figure 3 shows pulses-induced ring magnetization as a function of the delay time  $\tau$  and as a function of the field amplitude strength  $F_1$  of the first pulse ( $F_2 = 30$  V/cm). The generated net current  $I$  is inferred from Fig. 3 by noting that for the present ring a magnetization of 1 eV/T corresponds to a current of 8.9 nA. Thus, even for the weak pulses considered in Fig. 3, the induced peak magnetization is an order of magnitude larger than the conventional magnetization (typically  $\sim 0.45$  eV/T) which is measured in ballistic mesoscopic rings threaded by a magnetic flux [7] (measured persistent current is  $\sim 4$  nA). The direction of the induced magnetization depends on the polarity of the first pulse (cf. Fig. 3). Positive and negative values of  $F_1$  correspond to polarizations in the  $x$  and  $-x$  directions, respectively. Thus, a magnetization reversal is brought about by inverting the polarity of the first pulse; pulses with an alternating polarity are feasible experimentally [16,18]. The peak magnetization magnitude strongly depends on the time lag  $\tau$  between the pulses, a parameter that is well under control on a (sub)picosecond scale [16,18]. Hence, a desirable magnetic state of the ring could be realized experimentally with a high accuracy by tuning  $\tau$  and choosing the appropriate pulse's polarity.

The induced current and magnetization shown in Fig. 3 are nonequilibrium phenomena. The relaxation behavior to the (stationary) ground state is shown by the insets of Fig. 3 for two peak values of the induced magnetization. Once the current is triggered, it lasts for almost 100 ps. Recalling that the pulses last only for 1 ps, we conclude that the

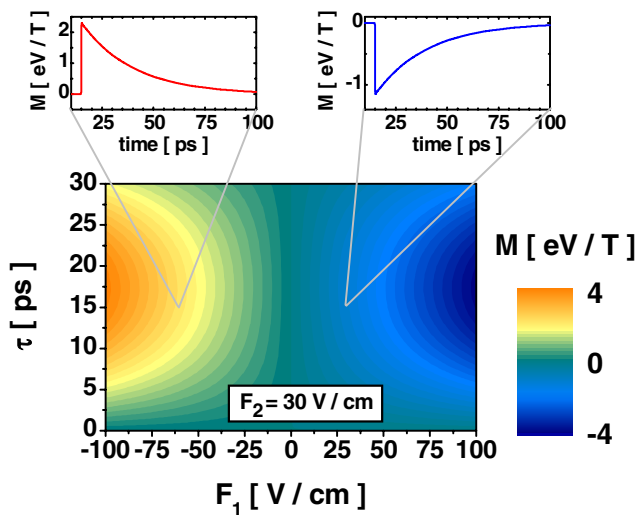


FIG. 3 (color online). Induced magnetization  $M$  as a function of the time delay  $\tau$  and the amplitude  $F_1$  of the first pulse. The amplitude of the second pulse is set to the value  $F_2 = 30$  V/cm. Positive and negative values of  $F_1$  refer to pulse polarizations in the  $x$  and  $-x$  directions, respectively. The upper left and right insets show for the time delay  $\tau = 15$  ps the time dependence of the magnetization for, respectively, the field amplitudes of  $F_1 = -60$  and  $30$  V/cm. The induced current is inferred from this figure by noting that for this ring a magnetization of 1 eV/T corresponds to a current of 8.9 nA.

induced current (and the magnetization) occur in an environment free of external fields. In addition, the buildup of the magnetization takes only a few picoseconds; i.e., phonons created on a longer time scale are hardly involved. We find the dependence of the induced current on  $F_1$  and  $F_2$  is generally nonlinear, except for the very weak field regime. The current temperature ( $T$ ) dependence is shown in Fig. 4 which evidences that  $I$  and hence  $M$  vary smoothly with  $T$  and persist at  $T$  as high as 50 K.

An experimental realization is achievable with current technology: The crossed, time-delayed strongly asymmetric pulses were recently utilized [17] for creating quarter-cycle circularly polarized pulses [29]. Also trains of pulses are feasible [18]. The use of a picosecond pulse train instead of a single pulse in Fig. 1 generates an averaged magnetization sustainable for the train duration. The values of induced magnetization are detectable by present magnetic imaging techniques [30–32], or by tracing the temporal change in the absorption properties (cf. [33]). Another possibility is to monitor the light emitted by the induced density oscillations [34].

The induced current can be utilized for several purposes. For example, short-time transport properties of ring structures can be monitored (via measuring the magnetization) without contacting the ring to diffusive electrodes. Hence, several problems encountered in conventional transport measurements can be avoided such as phase decoherence and the nonconservation of the number of particles when the ring is attached to diffusive leads. In addition, one may study the transition from the linear to the nonlinear response regime (in  $F_1$  and/or  $F_2$ ) by varying the pulse's strength. A further distinctive feature is that the current circulates in the absence of external fields (see Fig. 3). Hence, no complications arise due to an unknown voltage drop within the structure of an applied bias. Figure 3 also indicates that tracing the decay of the induced magnetization offers an insight into the decay behavior in the absence of external fields and offers a possibility to study the influence of various relaxation mechanisms that emerge at different time scales. Such a study is not feasible by using a ramped dc field because the field rise-up and switch-off times are well above the relaxation time.

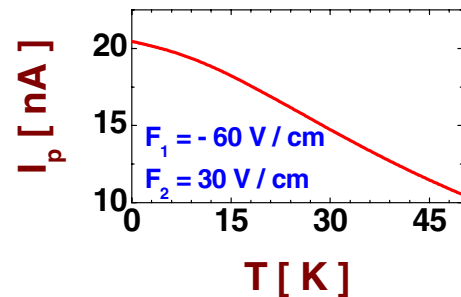


FIG. 4 (color online). Peak value of the induced current  $I_p$  as a function of the temperature  $T$  for a time delay  $\tau = 15$  ps between the pulses. The field amplitude strengths of the (1 ps) pulses are  $F_1 = -60$  V/cm and  $F_2 = 30$  V/cm.

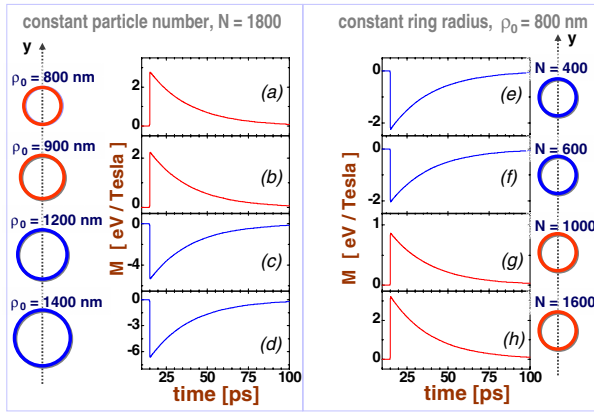


FIG. 5 (color online). The time dependence at  $T = 0$  of the magnetization induced by 1 ps pulses in an array of four non-interacting rings with a fixed particle number  $N$  and varying radii  $\rho_0$  [(a)–(d)] or with fixed  $\rho_0$  and varying  $N$  [(e)–(h)]. All rings are 100 nm wide, the field amplitude strengths are  $F_1 = F_2 = 80$  V/cm, and the delay time between the pulses is  $\tau = 15$  ps.

The schemes can also be utilized to generate and control dynamical collective magnetic phases in an artificially structured planar ring array, as shown in Fig. 5. Mesoscopic ring arrays (however interconnected) were realized experimentally in Ref. [35]. Irradiating an array of identical noninteracting rings creates a collective (nonequilibrium) ferromagnetic state. This state can be sustained or destroyed or the magnetization can be reversed depending on the pulse's duration, strengths, and polarities. As demonstrated in Fig. 5, various magnetically ordered states can be realized. For example, the magnetic moment of the individual rings in the array is tuned by varying the radii  $\rho_0$  or the particle number  $N$  [10] [see Figs. 5(a)–5(d)]. Upon the irradiation the array magnetization first builds up and decays in time, as shown in Fig. 5. Applying a pulse train to the array, a magnetization can be achieved that is sustainable on the time scale of the train duration. The latter is controllable experimentally.

In summary, we presented the first theoretical evidence and numerical results indicating that in ballistic ring structures (postpulse) current and magnetization are generated on a picosecond time scale by applying two linearly polarized unipolar pulses. The current temporal behavior and its magnitude and direction are controlled by the pulse's strengths and delay time. The current lasts as long as the coherence is preserved and up to temperatures of 50 K. We discussed various applications of this scheme and showed that the currents are detectable with today's technology.

- 
- [1] A. Kekulé, *Bull. Soc. Chim. Fr.* **3**, 98 (1865).  
 [2] Y. Imry, *Introduction to Mesoscopic Physics* (Oxford University Press, Oxford, 2002).  
 [3] F. Hund, *Ann. Phys. (Leipzig)* **32**, 102 (1938).

- [4] M. Büttiker, Y. Imry, and R. Landauer, *Phys. Lett.* **96A**, 365 (1983).  
 [5] L. P. Lévy, G. Dolan, J. Dunsmuir, and H. Bouchiat, *Phys. Rev. Lett.* **64**, 2074 (1990).  
 [6] V. Chandrasekhar *et al.*, *Phys. Rev. Lett.* **67**, 3578 (1991).  
 [7] D. Mailly, C. Chapelier, and A. Benoit, *Phys. Rev. Lett.* **70**, 2020 (1993).  
 [8] H.-F. Cheung, Y. Gefen, and E. K. Riedel, *IBM J. Res. Dev.* **32**, 359 (1988).  
 [9] Assuming  $\rho_0 \approx 0.5$  nm for benzene one requires then a magnetic field of  $|B| \approx \phi_0 / (\pi \rho_0^2) \approx 5000$  T.  
 [10] A. Fuhrer *et al.*, *Nature (London)* **413**, 822 (2001).  
 [11] A. Lorke *et al.*, *Phys. Rev. Lett.* **84**, 2223 (2000).  
 [12] R. J. Warburton *et al.*, *Nature (London)* **405**, 926 (2000).  
 [13] A. M. Weiner, J. P. Heritage, and E. M. Kirschner, *J. Opt. Soc. Am. B* **5**, 1563 (1988).  
 [14] A. M. Weiner, D. E. Laird, J. S. Patel, and J. R. Wullert, *Opt. Lett.* **15**, 326 (1990).  
 [15] M. M. Wefers and K. A. Nelson, *Opt. Lett.* **18**, 2032 (1993).  
 [16] D. You, R. R. Jones, P. H. Bucksbaum, and D. R. Dykaar, *Opt. Lett.* **18**, 290 (1993); N. E. Tielking, T. J. Benschky, and R. R. Jones, *Phys. Rev. A* **51**, 3370 (1995).  
 [17] T. J. Benschky, G. Haeffler, and R. R. Jones, *Phys. Rev. Lett.* **79**, 2018 (1997).  
 [18] A. Wetzels, A. Gürtel, H. G. Müller, and L. D. Noordam, *Eur. Phys. J. D* **14**, 157 (2001); M. T. Frey *et al.*, *Phys. Rev. A* **59**, 1434 (1999); B. E. Tannian *et al.*, *Phys. Rev. A* **62**, 043402 (2000).  
 [19] G. L. Carr *et al.*, *Nature (London)* **420**, 153 (2002); M. Sherwin, *Nature (London)* **420**, 131 (2002).  
 [20] T. Brixner *et al.*, *Phys. Rev. Lett.* **92**, 208301 (2004).  
 [21] A. Matos-Abiague and J. Berakdar, *Europhys. Lett.* **69**, 277 (2005).  
 [22] L. Wendler *et al.*, *Z. Phys. B* **100**, 211 (1996).  
 [23] K. B. Efetov, *Phys. Rev. Lett.* **66**, 2794 (1991).  
 [24] V. E. Kravtsov and V. I. Yudson, *Phys. Rev. Lett.* **70**, 210 (1993); O. L. Chalaev and V. E. Kravtsov, *ibid.* **89**, 176601 (2002).  
 [25] P. Kopietz and A. Völker, *Eur. Phys. J. B* **3**, 397 (1998).  
 [26] T. Chakraborty and P. Pietiläinen, *Phys. Rev. B* **50**, 8460 (1994); W. C. Tan and J. C. Inkson, *ibid.* **60**, 5626 (1999).  
 [27] C. Presilla and J. Sjöstrand, *Phys. Rev. B* **55**, 9310 (1997).  
 [28] J. M. Ziman, *Principles of the Theory of Solids* (Cambridge University Press, Cambridge, 1998), 2nd ed.  
 [29] Circularly polarized pulses could be employed; however, using two orthogonal, linearly polarized pulses allows utilizing their time delay and individual strengths as control parameters to achieve the desired current properties.  
 [30] *SQUID Sensors: Fundamentals, Fabrication and Applications*, edited by H. Weinstock (Kluwer, Dordrecht, 1996).  
 [31] I. K. Kominis, T. W. Kornack, J. C. Allred, and M. V. Romalis, *Nature (London)* **422**, 596 (2003).  
 [32] M. Pannetier *et al.*, *Science* **304**, 1648 (2004).  
 [33] R. Huber *et al.*, *Nature (London)* **414**, 286 (2001).  
 [34] A. Matos-Abiague and J. Berakdar, *Phys. Lett. A* **330**, 113 (2004).  
 [35] W. Rabaud *et al.*, *Phys. Rev. Lett.* **86**, 3124 (2001).